Proceedings of the 25th Jc-IFToMM Symposium (2019)
2nd International Jc-IFToMM Symposium
26th October 2019, Kanagawa

ENERGETIC ANALYSIS OF INDUSTRIAL ROBOTS FOR PICK-AND-PLACE OPERATIONS

FABRIZIO VIDUSSI
DPIA, University of Udine, Italy, vidussi.fabrizio@spes.uniud.it

PAOLO BOSCARIOL
DTG, University of Padua-Padova, Italy, paolo.boscariol@unipd.it

LORENZO SCALERA
Faculty of Science and Technology, Free University of Bozen-Bolzano, Italy, lorenzo.scalera@unibz.it

ALESSANDRO GASPARETTO
DPIA, University of Udine, Italy, gasparetto@uniud.it

ABSTRACT
In this paper a novel approach to the analysis of the energetic performance of an industrial robot is presented. The attention is focused on the energetic impact of two design variables which define a pick-and-place task: the choice of the trajectory planning algorithm and the location of the task within the workspace of the robot. An inverse dynamic model of the manipulator and the electro-mechanical model of the actuators are developed in order to estimate the energy consumption related to the execution of a basic motion task. The results are collected into energy consumption maps, which allow to investigate how the positioning of the task and the choice of the motion profile affect the energetic performance of the robot.

KEY WORDS: Energy saving, Trajectory planning, Task positioning, Pick-and-Place operation, SCARA robot

1. INTRODUCTION

In the last years, the growing energy demand and the increasing of environment awareness have shifted the focus of all engineering fields towards the research of new methods and solutions for energy saving. Especially in modern robotics, where high volumes of production and high speed operation are required, this trend has caused a great change in the mind-set of industries and researchers. As a proof of this, a large variety of techniques for the improvement of the energetic efficiency of industrial robots has been designed and tested in recent years, as presented in [9]. According to this, a first category of methods relies on hardware optimization, e.g. the selection of the most suitable robot model for a given task [10], the design of lightweight structures [3, 21, and 1], the use of systems for energy recovery [13] and the exploitation of robot natural dynamics [11, 14]. A second category relies on software optimization and in particular on the planning of energy efficient trajectories. Examples of such techniques can be found in [12], where a simple trajectory planning for energy saving of industrial machines has been developed, and in [15] where both energy and time optimal motion profile are analyzed for a 6 degree-of-freedom (d.o.f.) robot

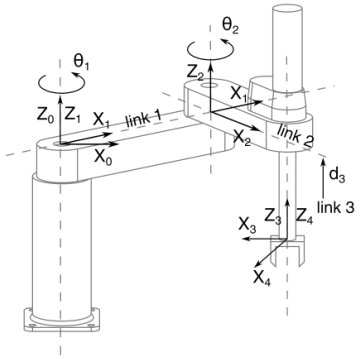

Fig. 1: SCARA robot structure.

performing a pick-and-place operation. In addition, a trajectory planning approach for energy saving of a redundant robotic cell has been designed in [4], whereas in [8] several point-to-point trajectories based on standard primitives have been adopted in order to reduce the energy consumption of 1 d.o.f. mechatronic systems. Other works [18, 20], focus on the enhancement of energetic efficiency of industrial manipulators by reducing the actuator effort thorough motion design.

From the literature it can be seen that several performance measures have been analyzed to characterize the behavior of industrial robots and can be divided in global and local measures. An example concerning the local measures is presented in [19], where a graphical visualization of several indexes computed for a SCARA manipulator is provided, whereas in [7] the optimal robot position is determined by defining and using task-dependent and direction-selective performance indexes for a parallel industrial robot executing a pick-and-place task.

The importance of these studies relies on the fact that local performance indexes can be useful to describe the relationship between the robot and the task definition, providing several guidelines in the choice of the areas of the workspace in which the performance of the robot increases [16]. This performance can be quantified by means of some measurement of dexterity, force or speed exertion capability, or manipulability, but currently there are, to the best of Authors' knowledge, no performance indexes strictly focusing on energy consumption.

With this final goal in mind, the aim of this paper is to provide a novel approach to the analysis of the energetic performance of a 3 d.o.f. SCARA robot. The energetic impacts of the path and trajectory planning are evaluated for a particular task, i.e. a common pick-and-place operation, as presented in [5, 6]. On the basis of the dynamic model and electro-mechanical model of the manipulator, the effects of the location of the task within the robot workspace on the overall energy consumption, as well as of the choice of motion profile, are investigated. For each motion law considered, numerical results provide energy consumption maps that are used to evaluate the energetic performance of the robot and to determine the optimal location of the task. Since this is a preliminary analysis, further and more detailed models will be implemented as well as actual data will be provided in future works in order to increase the reliability of the results obtained.

Table 1: Kinetic and dynamic properties of the SCARA robot.

Parameter	Joint 1	Joint 2	Joint 3
Link length	$0.35\ m$	$0.35\ m$	–
Link mass	$9\ kg$	$8\ kg$	$1\ kg$
Gear ratio	$1/80$	$1/50$	$1/50$
Motor inertia	$5 \cdot 10^{-4}\ kgm^2$	$4 \cdot 10^{-4}\ kgm^2$	$1 \cdot 10^{-4}\ kgm^2$
Viscous friction coefficient	$8 \cdot 10^{-4}\ Nms/rad$	$7 \cdot 10^{-4}\ Nms/rad$	$5 \cdot 10^{-4}\ Nms/rad$
Coulomb friction force	$2 \cdot 10^{-4}\ Nm$	$2 \cdot 10^{-4}\ Nm$	$2 \cdot 10^{-4}\ Nm$
Motor winding resistance	$0.39\ \Omega$	$0.39\ \Omega$	$1.67\ \Omega$
Motor back-emf constant	$0.16\ Vs/rad$	$0.16\ Vs/rad$	$0.12\ Vs/rad$
Motor torque constant	$0.28\ Nm/A$	$0.28\ Nm/A$	$0.21\ Nm/A$

2. DYNAMIC AND ELECTRO-MECHANICAL MODEL

The industrial manipulator under analysis in this work is a 3 d.o.f. SCARA robot, which is composed of two revolute joints and one prismatic joint (Fig. 1). The inertial properties of each link, motor and gear are reported in Table 1. The dynamic equation of motion, which represents the relation between joint torques $\boldsymbol{\tau} = [\tau_1\ \tau_2\ \tau_3]^T$ and joint variables $\boldsymbol{q} = [q_1\ q_2\ q_3]^T$, are obtained by using the Lagrangian formalism, leading to the following expression:

$$\boldsymbol{\tau} = \boldsymbol{M}(\boldsymbol{q})\ddot{\boldsymbol{q}} + \boldsymbol{C}(\boldsymbol{q}, \dot{\boldsymbol{q}})\dot{\boldsymbol{q}} + \boldsymbol{f}_v\dot{\boldsymbol{q}} + \boldsymbol{F}_c sign(\dot{\boldsymbol{q}}) \tag{1}$$

where $\boldsymbol{M}(\boldsymbol{q})$ is the mass matrix, the matrix $\boldsymbol{C}(\boldsymbol{q}, \dot{\boldsymbol{q}})$ accounts for Coriolis and centrifugal forces, $\boldsymbol{f}_v$ is the diagonal matrix of viscous friction coefficient, and $\boldsymbol{F}_c$ is the diagonal matrix of Coulomb friction forces. Assuming that brushless motors are used as in [4, 17], the relation between motor torques vector $\boldsymbol{\tau}_m(t)$ and motor current armature vector $\boldsymbol{I}(t)$ assumes the following form:

$$\boldsymbol{\tau}_m(t) = \boldsymbol{k}_t\boldsymbol{I}(t) \tag{2}$$

in which $\boldsymbol{k}_t$ in the diagonal matrix of the motor torque constants. Then, by using the motor armature model, the voltage drop $\boldsymbol{V}(t)$ across the stator windings can be represented as a function of the current $\boldsymbol{I}(t)$ and motor speed vector $\dot{\boldsymbol{q}}_{\boldsymbol{m}}(t)$ as:

$$\boldsymbol{V}(t) = \boldsymbol{R}\boldsymbol{I}(t) + \boldsymbol{k}_b\dot{\boldsymbol{q}}_{\boldsymbol{m}}(t) \tag{3}$$

in which $\boldsymbol{R}$ and $\boldsymbol{k}_b$ are the diagonal matrices of the stator resistance and the back-emf constants of each actuator, respectively. Finally, integrating the instantaneous electrical power over the time interval $t \in [t_i, t_f]$, the total energy E_{robot} absorbed by the robot motor during the execution of a generic operation in such time interval can be found:

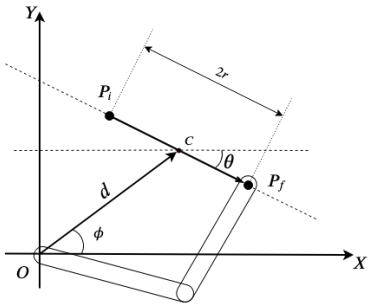

Fig. 2: Graphical representation of the parameters used to define the path.

$$E_{robot} = \int_{t_i}^{t_f} \boldsymbol{V}(t)^T \boldsymbol{I}(t) dt \; = \int_{t_i}^{t_f} \boldsymbol{I}(t)^T \boldsymbol{R}\, \boldsymbol{I}(t) dt \; + \int_{t_i}^{t_f} \dot{\boldsymbol{q}}_{\boldsymbol{m}}(t)^T \; \boldsymbol{k}_b \boldsymbol{k}_t{}^{-1}\, \boldsymbol{\tau}_m(t) dt \tag{4}$$

where the two integrals on the right highlight the Joule energy and the electro-mechanical energy. This second integral shows the most significant variations with respect to changes of the path parameters defined in the next section, whereas the first is far less sensitive to variations but has a higher impact. It has to be noted that, by varying properly the parameters of this model, several types of losses can be taken into account. For example, it is possible to increase the resistance values so as to include inverter losses, since these losses are proportional to the current. Similarly, the iron losses that depend on the motor speed can be considered by varying the viscous friction coefficient.

Since Eq. (4) represents the net energy balance of the robot within the time frame $[t_i, t_f]$, the current-voltage product can instantaneously take both positive and negative values, i.e. the electric power flow can be directed either from the grid to the motors or from the motors to the grid. However, this condition can be considered realistic only in the case of robots equipped with regenerative devices, which is a very uncommon situation for the most industrial manipulators. As a matter of fact, industrial robots are equipped with breaking resistors that are used to dissipate the excess of energy. Accordingly, the integral in Eq. (4) is computed taking into account only positive values of the instantaneous electrical power.

3. ENERGETIC IMPACT OF TASK POSITIONING

The dynamic model presented in the previous section is now used to analyze the relation between the positioning of the task in the operative space and the energy consumption related to the execution of that task. This analysis concerns a basic but common task, typically performed in pick-and-place operations, i.e. the point-to-point translation of the robot end-effector either along a straight line or an arc in the $\{X, Y\}$ plane, depending on the motion law adopted, as explained below. Referring to Fig. 2, such a task is represented by a vector that connects the starting point P_i to the final point P_f. The base of the robot performing that task is set on the origin O of the $\{X, Y\}$ reference frame. Then, given a fixed execution time and the total displacement $2r$, the task can be

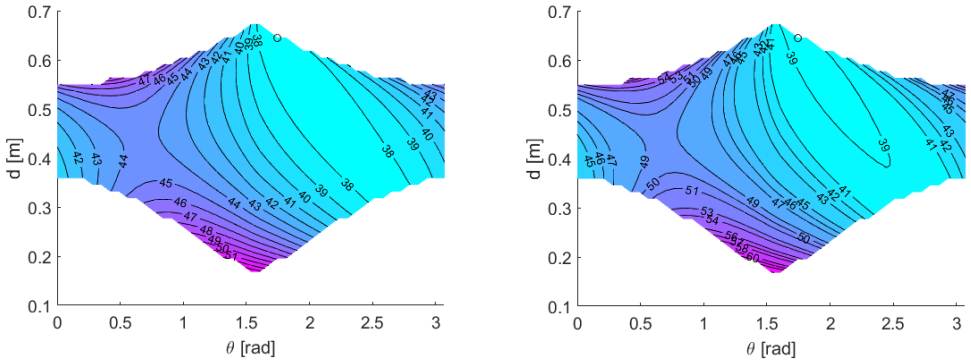

(a) (b)

Fig. 3: Energy consumption maps: third (a) and fifth (b) order motion profile in the joint space.

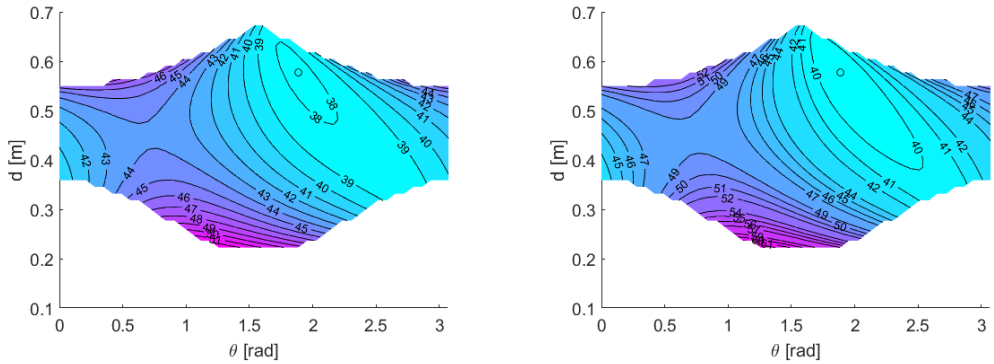

(c) (d)

Fig. 4: Energy consumption maps: third (c) and fifth (d) order motion profile in the operation space.

performed in infinite ways, as long as the initial point P_i and final point P_f are left free. Moreover, the choice of the task gains another degree of freedom if the motion law is left free as well.

Under these assumptions the path of the end-effector of the robot can be parameterized by three values: the real positive value d and the angle φ, which are the polar coordinates of the mid-point of the trajectory, and θ, which measures the orientation of the task within the workspace. Actually, on account of the angular isotropy of the SCARA, the parameter φ can be fixed to an arbitrary value, e.g. $\varphi = 0$, without affecting the energy consumption. Therefore, the parameterization can be limited to the distance d and the orientation θ of the path only. According to the dimensions of the links, the limits of the joints and the radial symmetry of the robotic configuration, the distance d ranges from $0.1\ m$ to $0.7\ m$, and the direction θ varies between 0 and π radiants. For all experiments the total displacement is set to $0.28\ m$ and the execution time is set to $0.8\ s$.

Concerning the motion law, four well-known algorithms are considered: the third and the fifth-degree polynomial profiles in the operation space, and the third and the fifth-degree polynomial

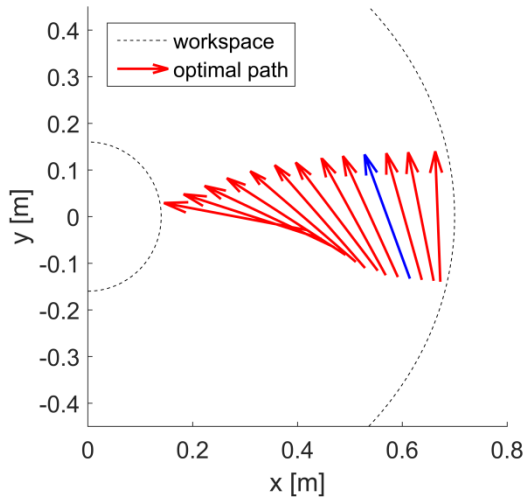

Fig. 5: Optimal path disposition varying the distance from the base; the absolute minimum energy path positioning is shown in blue.

profiles in the joint space [2]. In these last two cases the trajectory does not follow a straight line but instead an arc. The length of this arc has to be limited so as to avoid extreme deviations from the straight line length, which could lead to unreasonable energy consumption. In order to do this, a maximum arc length value related to the Euclidean distance between initial and final point is defined and the trajectories exceeding that value are considered unfeasible. At this point, the energy is calculated simulating the motion of the manipulator and varying the parameters d, θ in the ranges defined above. The values obtained are then collected in four maps, which correspond to the four motion laws, as shown in Fig. 3 and 4. Figure 3(a) shows a contour plot of the total energy absorbed by the robot when moving according to the third order polynomial profile in the joint space: each point of the map corresponds to specific values of θ and d and the total energy is expressed in Joule. Brighter colors are associated with tasks that require a lower energy to be performed, whereas white areas represent tasks which are unfeasible either because of workspace limitations or in case the relative trajectory exceeds joint position, speed and acceleration limitations as well as length limit. The analysis is repeated by using a fifth degree polynomial profile for computing the map in Fig. 3(b), and then by using the same profiles in the operation space to compute the contour plot in Fig. 4(a) and Fig. 4(b), respectively.

In each map the small black circle indicates the minimum energy consumption point: for all the maps this minimum is located away from the base of the robot and its position changes slightly between joint and operation space planning. Overall, the minimum lays in the area near $\theta \cong 2\,rad$ and $d \cong 0.6\,m$. According to the task parameterization already shown in Fig. 2, $\theta \cong 0\,rad$ corresponds to a radial motion from the base of the robot to the outer part of the workspace, whereas $\theta \cong \pi/2\,rad$ corresponds to a motion along the tangential direction. The comparison between the maps in Fig. 2 and 3 shows that the differences in the motion profile results in different energy absorption, as expected. In particular, for both the joint space and the operation space, the third order polynomial profile is the most effective as far as energy saving is concerned. Furthermore, planning in the joint space lead to more efficient trajectories, despite of the major length, and allows to extend the space of feasible solutions, given that the white area is slightly smaller. Regardless the small differences between the absolute values of energy consumption and

the dimensions of the unfeasible area, all maps present similar shapes, showing that both the most efficient points and the less efficient points are located roughly in the same areas of $\{\theta, d\}$ space. Therefore, it can be inferred that the total consumption related to a particular task is more heavily affected by the choice of the parameters of the path rather than by the specific design of the motion profile. As consequence, the location of the task within the workspace should be carefully defined whenever the choice is made available and the energy consumption of the robot is a critical parameter of the robotic operation.
The effect of the motion direction is more clearly understood by looking at Fig. 5: the red arrows represent the optimal path location for 13 distances from the base of the robot, and the blue arrow shows the overall optimal solution, which corresponds to $d = 0.57$ m and $\theta = 1.885\, rad$. Each arrow connects the initial point P_i to the final point P_f of the trajectory and refers to the third degree motion law in the operation space. According to the results of the analysis of energy consumption maps reported in Fig. 3 and 4, Fig. 5 suggests that a tangential motion is the best choice when operating in the outer part of the workspace, whereas a radial motion is the best choice when operating close to the base of the robot.

4. CONCLUSIONS

In this work a novel approach to the energetic analysis considering a 3 d.o.f. industrial robot has been presented. This analysis focuses on the estimation of the energy consumption of the robot in relation to the choice of the motion profile both in the operation space and in the joint space as well as the positioning of the task within the workspace. Firstly, the dynamical and electro-mechanical models have been defined. Secondly, given a planar translation task, two main parameters of the path have been defined and four motion profiles have been chosen. Next, the motion of the manipulator during the execution of the task has been simulated for each pair of parameters, computing the relative energy consumption by means of the previously defined model. Repeating this procedure for each motion profile, four energy consumption maps have been obtained. Analyzing these maps, it has been inferred that the positioning of the task has a more relevant impact on the energy absorption with respect to the choice of the motion profile. Therefore, the maps can be used to easily determine the optimal positioning of the task within the workspace in order to reduce energy consumption. Further developments of this work will also consider a more detailed model and experimental data to confirm the results obtained here.

REFERENCES

[1] Belotti, R., Caneva, G., Palomba, I., Richiedei, D., Trevisani, A., Model updating in flexible-link multibody systems, *Journal of Physics: Conference Series*, IOP Publishing, Vol.744 (2016), p. 012073.

[2] Biagiotti, L., Melchiorri, C.: Trajectory planning for automatic machines and robots, Springer Science & Business Media (2008).

[3] Boscariol, P., Gallina, P., Gasparetto, A., Giovagnoni, M., Scalera, L., Vidoni, R.: Evolution of a dynamic model for flexible multibody systems, *Advances in Italian Mechanism Science*, Springer (2017), pp. 533-541.

[4] Boscariol, P., Richiedei, D., Energy saving in redundant robotic cells: Optimal trajectory planning, *IFToMM Symposium on Mechanism Design for Robotics*, Springer (2018), pp. 268-275.

[5] Boscariol P., Scalera L., Gasparetto A., Task-Dependent Energetic Analysis of a 3 d.o.f. Industrial Manipulator, *International Conference on Robotics in Alpe-Adria Danube Region*, RAAD (2019), pp. 162-169.
[6] Boschetti, G., A picking strategy for circular conveyor tracking. *Journal of Intelligent & Robotic Systems*, Vol. 81 (2016), No. 2, pp. 241-255.
[7] Boschetti, G., Rosa, R., Trevisani, A., Optimal robot positioning using task-dependent and direction-selective performance indexes: General definitions and application to a parallel robot, *Robotics and Computer-Integrated Manufacturing*, Vol. 29 (2013), No. 2, pp. 431-443.
[8] Carabin, G., Vidoni, R.,Wehrle, E., Energy saving in mechatronic systems through optimal point-to-point trajectory generation via standard primitives, *Second Int. Conf. of IFToMM ITALY*, Springer (2018), pp. 20-28.
[9] Carabin, G., Wehrle, E., Vidoni, R., A review on energy-saving optimization methods for robotic and automatic systems, *Robotics*, Vol. 4 (2017), No. 6, p. 39.
[10] Chemnitz, M., Schreck, G., Krüger, J., Analyzing energy consumption of industrial robots. In: *Emerging Technologies & Factory Automation (ETFA)*, 2011 IEEE 16th Conference on, IEEE (2011), pp. 1-4.
[11] Goya, H., Matsusaka, K., Uemura, M., Nishioka, Y., Kawamura, S., Realization of high-energy efficient pick-and-place tasks of SCARA robots by resonance, In: *Intelligent Robots and Systems (IROS)*, 2012 IEEE/RSJ International Conference on, IEEE (2012), pp. 2730-2735.
[12] Ho, P.M., Uchiyama, N., Sano, S., Honda, Y., Kato, A., Yonezawa, T., Simple motion trajectory generation for energy saving of industrial machines. *SICE Journal of Control, Measurement, and System Integration*, Vol. 7 (2014), No. 1, pp. 29-34.
[13] Inoue, K., Ogata, K., Kato, T., An efficient induction motor drive method with a regenerative power storage system driven by an optimal torque. In: *Power Electronics Specialists Conference, 2008*. PESC 2008. IEEE (2008), pp. 359-364.
[14] Lu, G., Kawamura, S., Uemura, M., Proposal of an energy saving control method for SCARA robots. Journal of Robotics and Mechatronics, Vol. 24 (2012), No. 1, pp. 115-122.
[15] Paes, K., Dewulf, W., Vander Elst, K., Kellens, K., Slaets, P., Energy efficient trajectories for an industrial ABB robot. *Procedia Cirp*, Vol. 15 (2014), pp. 105-110.
[16] Patel, S., Sobh, T., Manipulator performance measures - A comprehensive literature survey. *Journal of Intelligent & Robotic Systems*, Vol. 77 (2015), No. 3-4, pp. 547-570.
[17] Richiedei, D., Trevisani, A., Analytical computation of the energy-efficient optimal planning in rest-to-rest motion of constant inertia systems. *Mechatronics*, Vol. 39 (2016), pp. 147-159.
[18] Shiller, Z., Time-energy optimal control of articulated systems with geometric path constraints. *Journal of dynamic systems, measurement, and control*, Vol. 118 (1996), No. 1, pp. 139-143.
[19] Tanev, T., Stoyanov, B., On the performance indexes for robot manipulators. *Problems of engineering cybernetics and robotics*, Vol. 49 (2000), pp. 64-71.
[20] Trigatti, G., Boscariol, P., Scalera, L., Pillan, D., Gasparetto, A., A new path-constrained trajectory planning strategy for spray painting robots. *The International Journal of Advanced Manufacturing Technology*, Vol. 98 (2018), No. 9-12, pp. 2287-2296.
[21] Vidoni, R., Gasparetto, A., Scalera, L., 3-D ERLS based dynamic formulation for flexible-link robots: theoretical and numerical comparison between the Finite Element Method and the Component Mode Synthesis approaches. *International Journal of Mechanics and Control* (2018).